Geomicrobiology Journal

ISSN: 0149-0451 (Print) 1521-0529 (Online) Journal homepage: http://www.tandfonline.com/loi/ugmb20

Quantitative 3-dimensional Image Analysis of Mineral Surface Modifications—Chemical, Mechanical and Biological

A. A. Gorbushina , A. Kempe , K. Rodenacker , U. Jütting , W. Altermann , R. W. Stark , W. M. Heckl & W. E. Krumbein

To cite this article: A. A. Gorbushina , A. Kempe , K. Rodenacker , U. Jütting , W. Altermann , R. W. Stark , W. M. Heckl & W. E. Krumbein (2011) Quantitative 3-dimensional Image Analysis of Mineral Surface Modifications—Chemical, Mechanical and Biological, Geomicrobiology Journal, 28:2, 172-184, DOI: 10.1080/01490451.2010.490077

To link to this article: http://dx.doi.org/10.1080/01490451.2010.490077

Published online: 24 Feb 2011.

Geomicrobiology Journal, 28:172–184, 2011

ISSN: 0149-0451 print / 1521-0529 online
DOI: 10.1080/01490451.2010.490077

Taylor & Francis
Taylor & Francis Group

Quantitative 3-dimensional Image Analysis of Mineral Surface Modifications—Chemical, Mechanical and Biological

A. A. Gorbushina,[1,2] A. Kempe,[3,4] K. Rodenacker,[5] U. Jütting,[5] W. Altermann,[6] R. W. Stark,[7] W. M. Heckl,[4] and W. E. Krumbein[2]

[1]*Freie Universität Berlin, and Department IV "Materials and Environment", Federal Institute for Materials Research and Testing (BAM), Berlin, Germany*
[2]*AG Geomicrobiology, ICBM, Carl-von-Ossietzky Universität Oldenburg, Oldenburg, Germany*
[3]*Science PR, München, Germany*
[4]*Department of Earth & Environmental Sciences, Ludwig-Maximilians-Universität, München, Germany*
[5]*Helmholtz Zentrum München, German Research Center for Environmental Health (GmbH), Institute of Biomathematics and Biometry, Neuherberg, Germany*
[6]*Department of Geology, University of Pretoria, Pretoria, South Africa*
[7]*Physics of Surfaces, Technische Universität Darmstadt, Darmstadt, Germany*

Three principally different mechanisms contribute to the wear-down process of mineral aggregates in sedimentary environments: (1) mechanical abrasion by forces of wind and water and by floating or saltating neighbouring grains, (2) chemical attack and dissolution by fluids, and (3) physical bioerosion and chemical biocorrosion. It is however, difficult to attribute the specific surface changes to specific environments and processes. Quartz sand grains from subaerial and subaquatic environments were analysed by atomic force microscopy (AFM) for traces of natural and experimental aeolian, aquatic and biological wear-down processes. Quantitative topographical parameters of surface alterations were extracted from topography data by non-linear methods derived from digital image analysis. These parameters were examined by multivariate statistic, yielding three well-distinguishable groups. Morphological surface alterations dominated by subaerial, subaquatic and by biological impact could be differentiated. The method may also be used for the detection of aeolian, subaquatic, and biological modification of sedimentary grains and rock surfaces in extraterrestrial environments, and for assessment of environmental damage on monuments and buildings.

Keywords sediment grain corrosion, chemical grain pitting, biological grain pitting, aquatic grain corrosion, biopitting, weathering, surface analysis, nano-structure of grain and mineral surfaces

Received 1 August 2009; accepted 25 March 2010.
The authors acknowledge support by DFG grants Kr 333/30-1, Go 897/2-1,2 and BMBF grant 03G0709A.
Address correspondence to A. A. Gorbushina, Free University of Berlin and Federal Institute for Materials Research and Testing (BAM), Department IV Materials and Environment, Unter den Eichen 87, D-12205 Berlin, Germany. E-mail: anna.gorbushina@bam.de

INTRODUCTION

Rock, mineral grains and idiomorphic crystal surfaces exposed to atmosphere and climate are subject to biologically, chemically and physically induced morphological changes. Characteristic surface structures are generated this way, depending on rock or mineral type, depositional setting, climatic conditions, exposure time, and the associated microbial colonisation. The most characteristic and morphologically well defined are those structures produced through mechanical abrasion, by forces of wind, water or ice and by bulk sediment transport processes (Kuenen and Perdok 1962; Krinsley and Doornkamp 1973 and references therein). The second characteristic but less well-defined process is that of purely chemical aggression of watery solutions on mineral surfaces resulting in crystallographically oriented dissolution (Marshall 1987, e.g., and references therein) and possibly subsequent healing-precipitation patterns (compare Tietz 2006).

Among the emerging surface morphotypes (microrelief or micromorphology) well-defined characteristic structures are produced by epilithic and endolithic subaerial or subaquatic microbial biofilms and networks (biodyction). Crater-shaped biopittings, bioerosion fronts, biochipping and exfoliation are the most prominent biogenic structures recorded on desert rocks and building surfaces. Biopitting, however, occurs also in subaquatic systems, on siliciclastic sedimentary grains (Brasier et al. 2006); on volcanic grains and lava (Furnes et al. 1999) and on carbonate or phosphate grains and rocks (Flügel 2004; Zhang and Pratt 2008) and other minerals (Benzerara et al. 2005). It has been traced throughout the entire geologic record of sedimentation and life, e.g., cortoidal clasts in Archean carbonates (Altermann

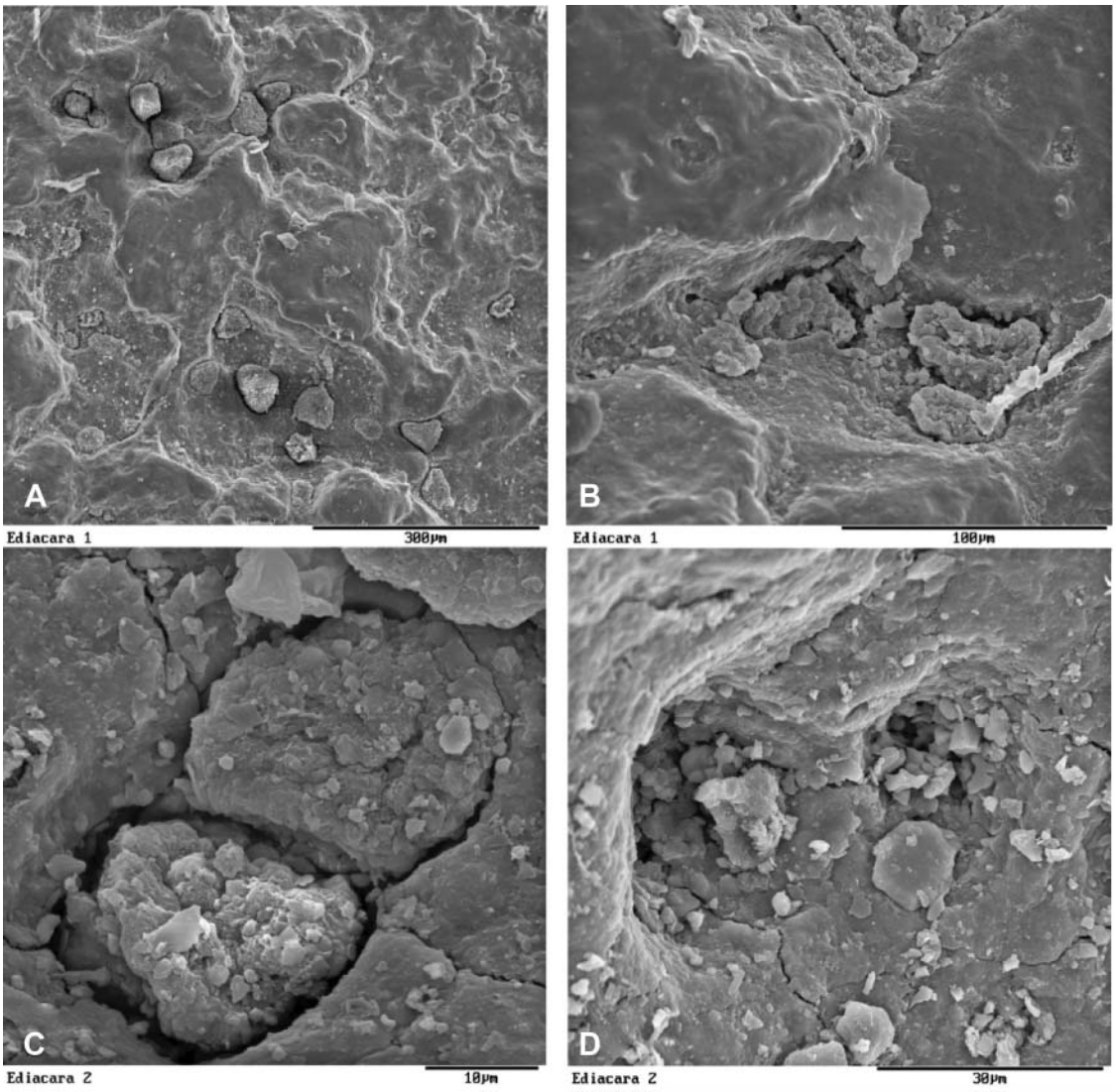

FIG. 1. (A) Cherty quartzite of the Ediacara Formation with about 20 microcolonies of black yeast etching biopits into the hard rock. Smooth surfaces exhibit polishing through wind. (B) Enlarged surface area showing smooth rock, biofilm slime cover (EPS), colonies covered with EPS and dust particles and one colony showing individual cells of black yeast. (C) Two adjacent black yeast colonies with particles attached to EPS deeply incised into the rock. (D) Ediacara quartzite after maceration with Eau de Javelle which eliminated almost all organic material of the rock boring black yeast.

and Herbig 1991), biocorroded pillow rims and hyloclastites (Furnes et al. 2004) or Archean cortoidal quartz grains (Brasier et al. 2006). Structures that modify the original relief of grains, minerals and rocks can thus be classified as biogenic or abiogenic structures.

Some examples of biopitting are illustrated in Figures 1 and 2, using SEM images of Ediacara rock samples and North Sea sand grains. Biogeomorphogenetic changes of rock and soil surfaces were described initially in the last century. Krumbein (1969) and Krumbein and Jens (1981) pioneered this work depicting microbial erosion and biopitting in the Negev desert (Israel). Danin and Garty (1983) described further examples of biopitting in the Negev desert. More recently the biocorrosion structures gained importance as possibly traceable, fossilized leftovers of ancient life on Earth, Mars and other planetary bodies, within the reach of robotic missions.

They were multiply and controversially discussed from recent and ancient terrestrial deposits and from different points of view (e.g., Krumbein 2008; Altermann et al. 2009). The importance of the role of microbiota and microbial mats in siliciclastic deposits, influencing preservation of grain size and morphology and of sedimentary structures, were recently emphasised by Brehm et al. (2005) and by Schieber et al. (2007 and references therein).

To the best of our knowledge, the term biogeomorphogenesis was first used by the group of Viles and Goudie at Oxford (Viles 1988; Viles and Goudie 2000) to describe morphogenetic surface changes caused by microbiota in the aquatic

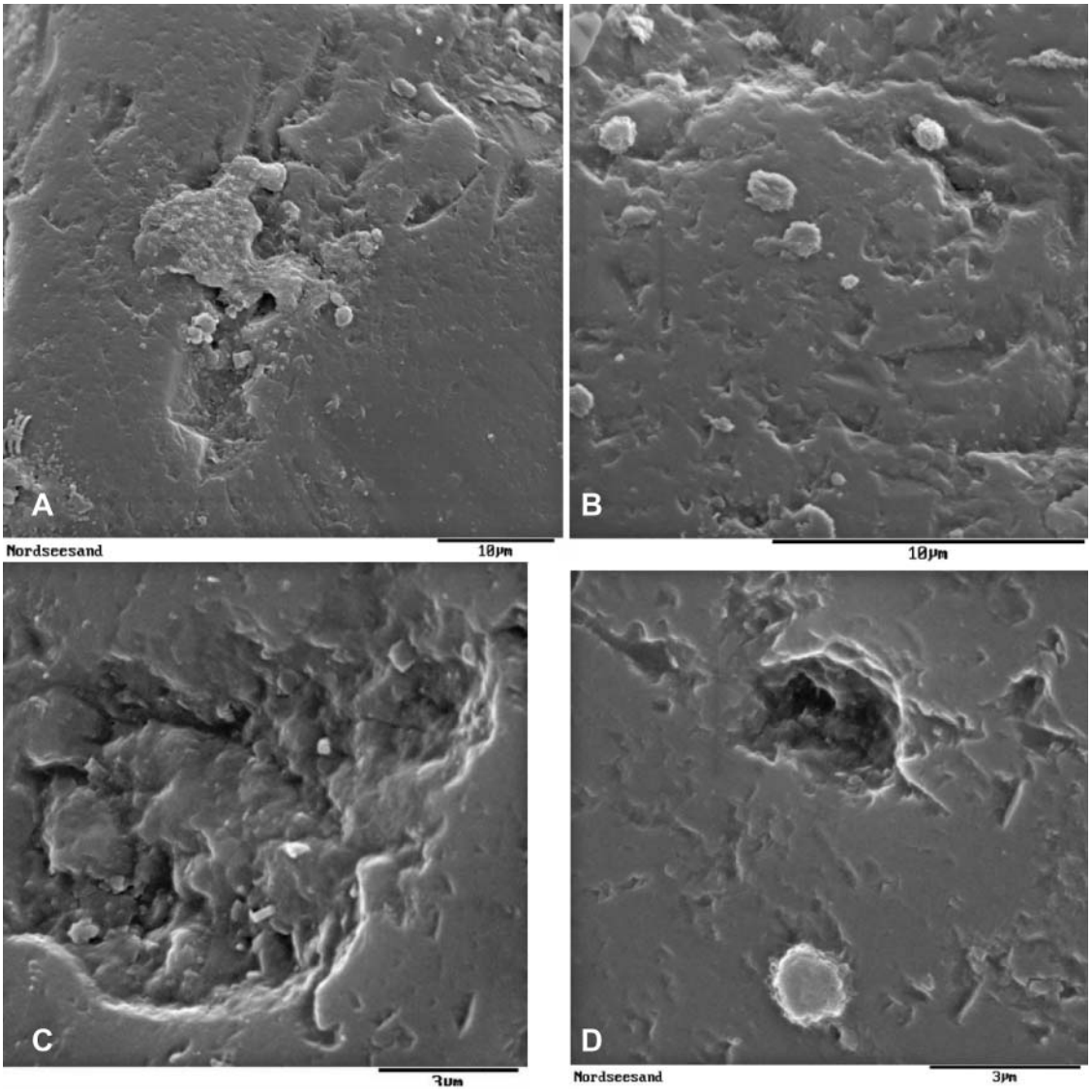

FIG. 2. (A) North sea quartz grain with biofilm and cell network. (B) North sea quartz grain showing individual cells etching round and smooth structures. (C) Biopit produced on North Sea sand grain after maceration of the grain with Eau de Javelle. Clearly visible smooth bioetching and triangular cutting traces by grain to grain collisions. (D) Unetched sample with cell creating biopit. Above the cell an empty pit where a previous growth was washed out cut away by grain to grain contact. Triangular collision traces on surface visible.

and terrestrial environments. Krumbein and Gorbushina (1995), Gorbushina and Krumbein (2000) and Fuxing et al. (1993) have applied this concept to many different environments, partially headed under the terms "Biokarst" and "Biopatina" (Krumbein 2003). Staley et al. (1982) were the first to describe the morphogenetic importance of black microcolonial fungi on rock surfaces in the Mohave Desert. Gorbushina and Krumbein (2000) and Carter et al. (2001) simultaneously suggested that such investigations of the biomorphogenetic potential of microbiota may help to detect life or life remnants also in extraterrestrial environments. It is assumed, that traces of extinct living forms on planets such as Mars, can probably be derived by the modelling of rock-surface changes initiated and created by e.g., endolithic microbial communities (Krumbein 2008; Altermann 2009).

The main features approached in the present work are biopittings, as compared to pitting by wind and wave generated grain-to-grain collisions (Krumbein 1969; Krumbein and Jens 1981; Krumbein et al. 1991, 1998; Gehrmann et al. 1988a; Gehrmann 1992; Gehrmann and Krumbein 1994; Steringer and Krumbein 1995, 1997; Eppard et al. 1996; Dornieden et al. 1997, 2000; Gorbushina et al. 1993; Gorbushina and Krumbein 2000; Gorbushina et al. 1996, 2001; Kempe et al. 2004). Abiogenic corrosion and mineral and grain surface modification has been used much more widely then biopitting structures in the past, for palaeoenvironment and palaeogeographic reconstruction (e.g.,

Fortuin 1984; Altermann 1986); and has been meticulously investigated in nature and in laboratory experiments since at least mid 20th century (e.g., Callieux 1952; Kuenen 1959a, 1959b; Krinsley and Doornkamp 1973; Whalley and Krinsley 1974, and references therein).

The term "pitting" as a synonym for smaller or larger crater-shaped cavities forming in many rocks and mineral grains is derived from "pit mining." The definition according to geological nomenclature is: "small indentation or depression left on a rock surface as a result of some corrosive or eroding process such as etching or differential solution" (Bates and Jackson 1990). We have identified and defined biopitting as the sole source of these crater shaped cavities in many places, publications leading back to the Book of Moses (Levithicus), quoted by Krumbein and Jens (1981). Krumbein (1969); Gehrmann et al. (1988a, 1988b) and others have now fully elaborated the processes of biological micro-, meso- and macropitting, as being caused mainly by endolithic and epilithic lichens and free living specialised microorganisms (e.g., *Geodermatophilus*, *Chroococcidiopsis* and black yeast-like rock fungi). Danin et al. (1982); Danin and Garty (1983) have substantially added to the knowledge on biopitting. On limestone and marbles biopitting, chipping, cracking and fissuring are frequently seen, of which the corrosion by biopitting dominates. Gehrmann et al. (1988a, 1988b) have classified these characteristic holes and cavities into three size groups namely (1) micro-, (2) meso- and (3) macropitting of the rock or mineral grain surface.

Of these, both, micropits and mesopits were identified, upon maceration, as produced by the activities of epilithic and endolithic lichen. The specific pitting pattern indicated by the penetration of bundles of hyphae (mesopits) as well as by individual hyphae (micropits) is clearly visible on the rock surface. When the pits fuse, they may produce a kind of of alveolarization structure on the surface, but of a significantly different morphology then individual meso- or micropits (Krumbein 1969). In view of the general importance of this biogenic process patterns a tentative classification is given here:

1. Micropitting. In this case etching figures are observed that correspond closely to the pencil etching described by mineralogists. This type of pitting is discussed as chemical or biological and describes deep vertical holes within minerals, which resemble deep pencil incisions in soft material. The holes are very deep and disregard any crystal lattice or mineral cleavage structure (Civan 2006). They are caused by individual cells and trichomes or mycelia of bacteria or fungi and are only visible under the scanning electron microscope. The diameter of these micropits is between 0.5 and 20 μm. The depths can reach several micrometers and even hundreds of micrometers in special cases.
2. Mesopitting. In this case chiefly etching figures of the fruiting bodies of endolithic lichens are dealt with. In some cases, also the "nap-shaped" grooves of cyanobacteria and/or algae underneath a crustose lichen film can form mesopits. They form little pockets which, upon further biocorrosion or chemical weathering have the shapes of half-ellipsoids or lensoidal cavities. Fungal hyphae can be associated with this pitting type as well. The diameter of the craters is usually between 20–800 μm.
3. Macropitting. These are the typical pits and scars clearly visible on many rocks, in various climates but especially in the spray zone of waves or in dew exposed desert environments and most importantly on many statues and marble monuments all around the Mediterranean but also on a smaller scale in e.g., Potsdam and other northern areas. A schematic model of pit formation has been published earlier (Krumbein 1987). Here, we are dealing with the not yet sufficiently analysed fusion of several pits in which fractal physical patterns may also play an important role. Some of the macropits are also derived from deeply incising epilithic lichen of ill-defined taxonomy. The macropits usually range in diameter from $\sim$1 mm to maximally 2 cm and depths between 1 and 5 mm.

From the point of view of evolutionary biology and for exobiological considerations, the understanding of ancient, fossilised biopitting recorded from different types of rocks is important. Stroncik and Schmincke (2002, and references therein) briefly reviewed microbial pitting in volcanic glass, related to palagonitization, and mentioned that at the glass alteration interface due to glass palagonitization, tubular structures may be interpreted as produced by endolithic microbial activity. Such pitting observed in ancient rocks, back to the Archean, consist of microtubules of up to 200 μm in length and up to 10 μm in diameter. However, in experiments, lithophilic or endolithic bacteria dissolving rock surfaces as a result of their metabolic process, in the search for nutrients and electron donors, produce typical pitting of μm size, usually of shallow, irregular, saucer shaped morphology (e.g., Thorseth et al. 1995; Einen et al. 2004). The observed 1–9 μm diameter and up to 200 μm long tubes in e.g., pillow rims and submarine volcanic rocks (hayloclastites, palagonite) (Furnes et al. 2004) are not an energetically effective constellation for rock surface colonisation, as bacterial colonies utilising the mineral substrate as the source of food, should prefer to spread along a surface rather than "burrow" deep and narrow tubes into the rock, where the exchange with the environment would be ruled by capillary physics.

It has been suggested that such microtubules may represent degassing and alteration (magma-water reaction) structures in volcanic rocks, later occupied by microbial consortia (Altermann 2007). The problem of microbially produced microtubules in ancient rocks and mineral grains seems thus not yet resolved.

Summarizing, biopitting is regarded as a biological process producing chemically and physically typical morphotypes, which are related to subaquatic or subaerial biofilm, made of consortia of bacteria, cyanobacteria, free living fungi, and

lichens. It remains however difficult to differentiate biopitting and the various other surface alteration processes. Usually, microscope images of the grain surface are used to infer the dominating process. So far, image interpretation is based on the experience and knowledge of the scientist. To obtain additional information on a more objective basis, statistical parameters are required that characterize the grain surface and its surface morphology. Such a statistical tool should allow one to discriminate grains from distinct environments.

To this end, we suggest a digital processing image approach based on non-linear transformations. Input data are the three-dimensional relief as measured with an atomic force microscope (AFM). From this surface map we derive statistical parameters, which allow us to discriminate characteristic surface morphologies. The work discussed here aims at differentiating between aeolian-physical, aquatic-physical, chemical and biogenic lesions, produced on sand grains exposed to wind, water, and to biological agents. Such a statistical data analysis procedure can help to derive a set of criteria to differentiate between the processes of mineral surface modifications. The main goal of the study was to apply statistically sound techniques to differentiate between images of biogenic and abiogenic surface changes in the natural sedimentary environment.

MATERIAL AND METHODS

Sample Locations

Spanish Coast. Samples were taken from the playa area between Zahora and Los Canos de Meca, Gibraltar, Spain. The prominent outcropping rock in this area is a cross bedded marine quartz sand-stone containing a fossil mollusc fauna. Sand detritus from the rock forms a beach area, several hundred meters in width, that is structured in a subtidal (1), an intertidal (2) and a supratidal (3) zone. The subtidal zone is submersed at all times, thus only subject to aqueous erosion. The dominant type of deposition is wave-ripple and current-ripple cross bedding. In the supratidal zone however, a seasonal lagoon is formed during winter time, that receives the directly precipitated rain fall and water drained from the nearest surroundings. In how far saline and phreatic groundwater contribute to the lagoon formation is not known.

The intertidal zone is regularly flooded at high tide and exposed to wind at low tide. In the intertidal zone sand grains are deposited in a mixture of aeolian ripples and dunes and marine ripple cross beds regularly superimposed but also eroding each other. This complicated system is crosscut by fluvial channels that carry water from inland brackish pools to the waterline and vice versa. The supratidal zone is subject only to aeolian influence and is occupied by aeolian sand dunes and coarser interdune lag deposits. Occasional storm flooding of the low areas during high tides however can not be ruled out. Samples were taken (1) from below the low tide waterline in the subtidal zone, called subaquatic, (2) from cross-bedded loose sand in the intertidal zone, far from any channel structure, and (3) from the top of a sand dune in the supratidal zone, called subaerial (Figure 3).

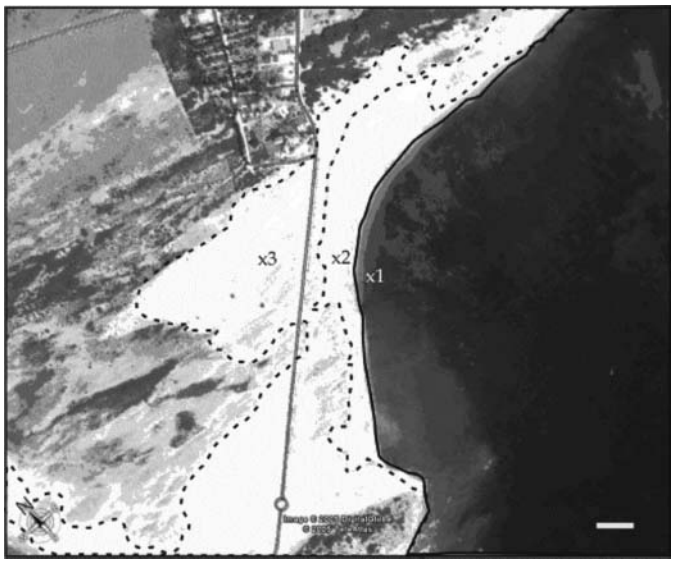

FIG. 3. Gibraltar beach area with 3 deposition zones (*Lat: 36.1857N; Lon: 6.0205W*): (x1) subtidal/subaquatic, (x2) intertidal, (x3) supratidal/subaerial. Scalebar 100 m.

German North Sea coast. Samples were taken from the intertidal flats of the Wadden Sea between Wilhelmshaven and Mellum (Krumbein et al. 1994, 2003). Microbial biofilm and mats cover extended areas in this shallow marine intertidal system. Due to the tidal cycle the water cover of the biofilm systems usually is less than 6 hours twice a day. Fine, sand of a grain size between 150 and 350 μm was selected for laboratory incubation in order to accelerate biofilm growth and potential microbial attack on sand grains (Brehm et al. 2005). Grains, which were incubated with biofilm material, were compared to those kept under sterile conditions under seawater cover. Data from this experiment are listed under Wadden, North Sea in Tables 1 and 3.

Specimen Preparation

From each sample, grains with a shape that exhibited some smooth spots at the micrometer scale and a shiny appearance under a low-power binocular were selected. The reason for this

TABLE 1
Gathered digital image data from AFM with totally examined area

Code	Type	Location	Images	Resolution [nm/pixel]	Total Area [μm^2]
1	subaquatic	Gibraltar	49	58.65	19600
2	intertidal	Gibraltar	$72 = 45 + 27$	58.65	28800
3	subaerial	Gibraltar	68	58.65	27200
4	Wadden	North Sea	62	58.65/39.1	24800

selection that bears some danger of missing the most typical surfaces, especially of mechanically abraded grains, was the effort to avoid highly rough surfaces that are difficult to access with an AFM (Kempe 2003). Previous investigations have shown however, that such risk can be minimised by careful selection (Kempe et al. 2004). Grains were glued with their roughest side onto a copper wire, 10 mm long and 0.5 mm in diameter, with Pattex gel superglue (Henkel, Düsseldorf, Germany) for soldering on a 1 cm x 1 cm copper sheath that was mounted on the scanning stage with a vacuum pump.

Sand grains were submersed for 5 min in 10% H_2O_2 solution, one day after mounting, to remove all organic material. The specimens were rinsed with distilled water and cleaned in an ultrasonic bath for 5 min, then dried with a nitrogen gun. Specimens were stored in a exsiccator. Bending the wire provided a freely accessible smooth side for topography imaging by AFM. Areas of interest were selected and rotated to the topmost position. In the case of the Gibraltar samples smooth sides-, in the case of the North Sea samples colonised areas were selected. The orientation of the specimen was kept constant after that to ensure reproducibility.

Three-dimensional Imaging of Sand Grain Topography

For each specimen the selected areas of interest and orientation were realigned with help of the optical photograph. The AFM-instrument is equipped with an integrated dissecting microscope. With the aid of this tool representative "mechanical" and "biogenic smooth" lesions were selected for AFM imaging. Several AFM images were obtained on different spots within the area. Images were taken using a Veeco Atomic Force Microscope Dimension (Veeco, Mannheim, Germany), equipped with a tube-piezo scanner with a maximum planar range of 100 μm in each of the planar (x, y) directions and a maximum vertical (z) range of 6.5 μm. The images were acquired utilising the intermittent contact mode in air (using NCHRW-reex coated and SSS-NCH cantilevers from Nanosensors, Neuchatel, Switzerland).

The choice of imaging condition, which was selected from various tested AFM modes, produced the clearest images and caused the least destruction of the cantilevers at the tapping mode. For each grain, square images with a 60 μm scan range were taken. The resolution was set to 1024 measure points per line. Since sand grains have relatively rough surfaces for AFM scanners, the scanning speed was limited to 10 μm/s, and the size of the studied area was 60×60 μm^2 or less, in 90% of all specimens. The reason for this limitation is caused by the curvature of the grain surface, the maximum amount of vertical extent of the relief increased as the analysed area increased. Scanning speeds faster than 10 μm/s would result in height jumps of the cantilever and lateral distortions at steep relief features. The scanned images represent 3 dimensional, topographic maps with a resolution of 58.5 and 39.1 nm/pixel. For analysis, the scanned images were tiled to 20 μm sized images. Each tiled image was subjected to a first-order plane set correction (SPIP, Vers. 3, Imagemetrology, Hörsholm, Denmark).

RESULTS

Overview

Only a small but representative selection of the three microscopic techniques (LM, SEM, AFM) is depicted in Figures 1 and 2. More and very characteristic structural and morphogenetic implications may be derived from the literature given in the introduction. As for the mechanical erosion patterns on mineral grain surfaces, it has to be noted, that crystal cleavage characteristics, even down to the Angstrom level of crystal lattices, show clear geometries and sharp angles either in relation to the crystal faces and classes or in relation to physical impact comparable to cracks by bullets on walls of houses under war fire, hits by hammer and chisel or rapid and forceful grain to grain collision in wave motion or desert wind.

This is clearly visible in Figures 2c and 2d. Biopitting on the other hand has either a specific jigsaw pattern or very smooth borders often irrespective of and independent from the crystal lattice and grain hardness. These very smooth alteration traces are clearly distinguishable from physical impact as seen in Figures 1 and 2. Very smooth and often wavy indentations near and around microorganisms or places where microorganisms lived, are characteristic of chemical biopitting. Physical biopitting produces rather jigsaw like zigzag patterns.

These microbially produced smooth, wavy or zigzagging patterns, at or near microbial attachment and penetration sites, reach orders of magnitude below the size of the microorganism producing them. The visible traces (in SEM and AFM) reach levels between 100 and 250 nm (Brehm et al. 2005). In the following the focus is mainly on classification results and mathematical approaches to nano- and microscale morphogenetic features of surfaces which are not or rarely visually discriminatable. In order to quantify these morphological observations and to develop objective criteria we discuss a mathematical procedure to classify surface alterations from topographic AFM data.

A typical microscope image based on topographic AFM data is outlined in three different representations in Figure 4. The quantitative characterisation of such data is either object-oriented or synthetic. The first measures properties of before hand defined and recognisable objects such as holes, mountains, saddles, the other models the surface by typically regular structures under different scales. According to the large differences of surface structures in occurrence and size of the samples, we have applied only synthetic measurements and focus on structures of 100 – 1000 nm spatial size only.

From visual observation of the samples, structures less than 1μm in diameter cannot be defined or recognised as objects (see Figure 4). Typically synthetic measurements are applied to residues of smoothing operations, so to say, an overlaid variability. With other words, the image is dissociated into a smooth and a variable compartment similar to signal decomposition. From the latter quantitative features were extracted only.

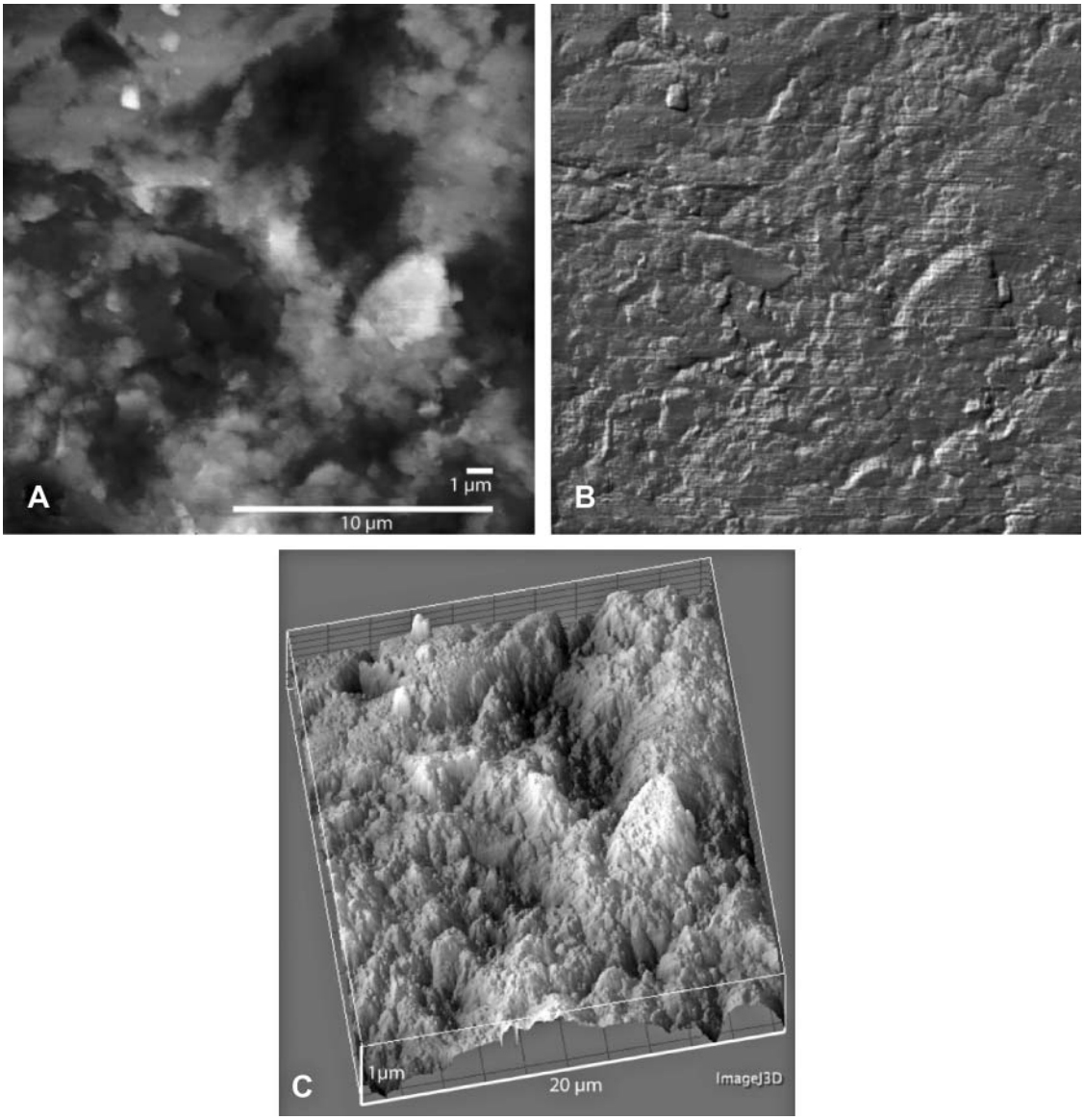

FIG. 4. AFM height map represented as intensity (A) with brightness showing height, pseudospatial or embossed (B) and rendered (C) images (C prepared with ImageJ, (Rasband 2009) and ImageJ3D).

Image Analysis

To extract this variable compartment, the variations, from the surface, we applied non-linear transformations for a better control of sensitivity and to avoid edge effects, as follows. Let f be the original AFM height map:

- non-linear Gaussian (*nlg*) (Aurich and Weule 1995; Winkler et al. 1999)

$$f_{nlg} = f - nlg(f, \sigma_x; \sigma_y; \sigma_z)$$

with standard deviation $\sigma_x = \sigma_y = \sigma_z = 120$ nm of smoothing Gaussian in $x; y; z$ and

- mean opening-closing (mathematical morphology) (Serra 1982; Rodenacker and Bengtsson 2003)

$$f_{OF} = f - 1/2(f^{Br} + f_{Br})$$

with B_r equal to a spherical structural element of radius $r =$ 1000nm, op^{Br} the closing ($op^{Br} = (op \oplus B_r) \ominus B_r$) and op_{Br} the opening operation ($op_{Br} = (op \ominus B_r) \oplus B_r$) for any operand op. The kernel sizes for smoothing, standard deviations $\sigma_{x;y;z}$ for *nlg* and radius r for opening and closing were chosen related to the considerations above.

The operation *non-linear Gaussian* is illustrated in Figure 5 in intensity and in embossed versions. The height map is

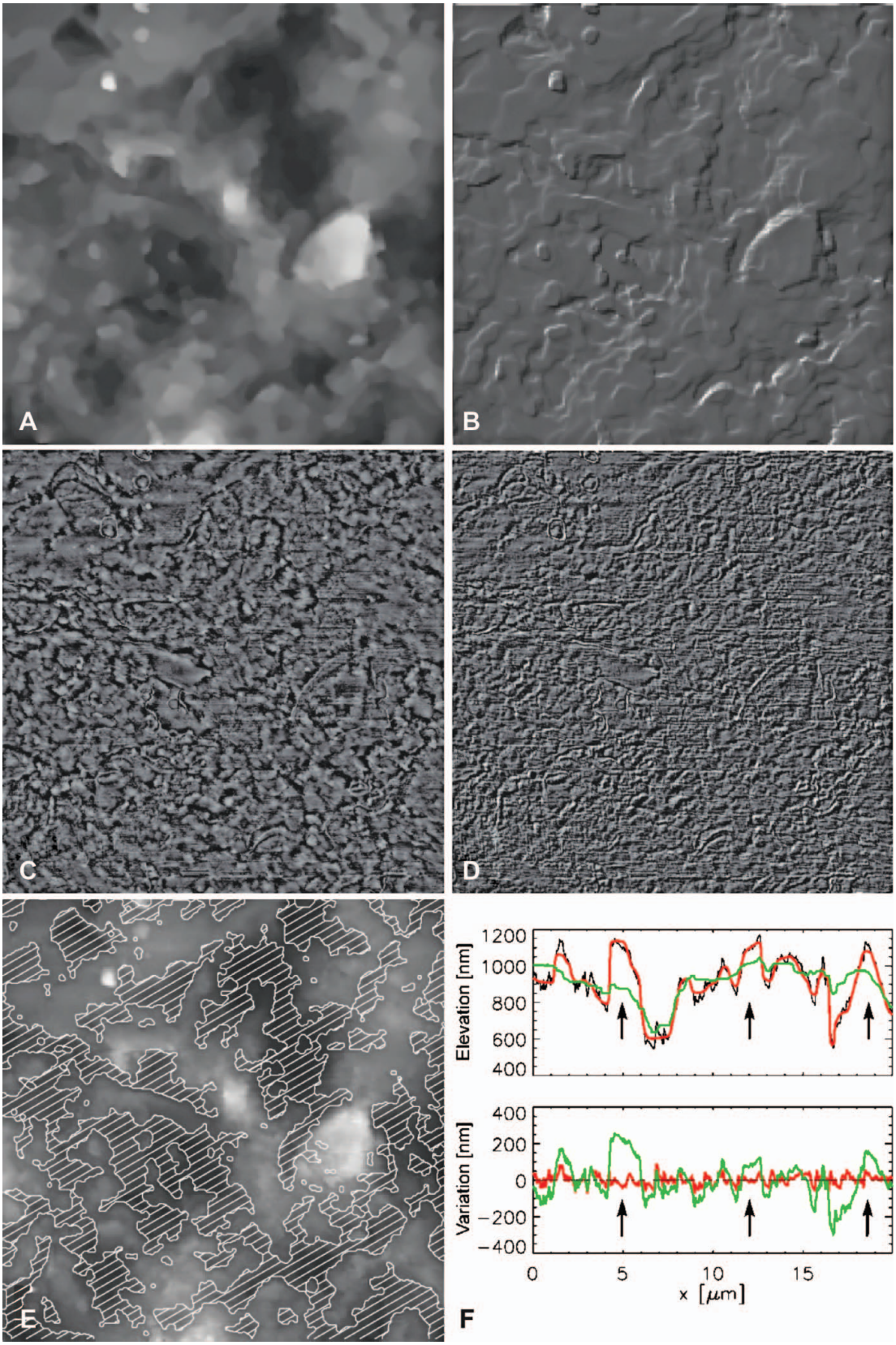

FIG. 5. Transformations *nlg* (A, B) and residues (small scale variation height map) f_{nlg} (C, D) represented as intensity and pseudo-spatial or embossed images. Bright areas correspond with higher locations. (E) The original image hatched by the dark mask M_d of depressed regions. (F) Upper graph shows one scanline of the height map with the transformations *nlg*(f, σ_x, σ_y, σ_z) in red and 1/2 ($f^{Br} + f_{Br}$) (*OF*) in green. Lower graph shows the scanline of the residues, f_{nlg} in red and f_{OF} in green.

nlg (A, B) smoothed. The residues (C, D) show only small-scale variations and the absence of larger, deeper or higher structures recognisable in Figure 4. In Figure 5F, one scan line is displayed with the respective transformations and residues. The different sizes of the smoothing kernels for *nlg* and morphology are clearly visible (arrows). The upper graph shows one scanline of the height map with the transformations $nlg\,(f;\sigma_x;\sigma_y;\sigma_z)$ in red and $\frac{1}{2}\,(f^{Br} + f_{Br})$ (OF) in green. The lower graph shows the scan line of the residues, f_{nlg} in red and f_{OF} in green.

Features

The residue images f_{nlg} and f_{OF} are analysed by first-order statistics for the whole region as well as for a partition of the image into positive and negative altitudes called dark ($M_d = f_{OF} < 0$) and bright areas ($M_b = f_{OF} \geq 0$) (Rodenacker and Bengtsson 2003). The dark area is outlined in Figure 5E hatched. This distinction allows the separate analysis of surface structure in sinks (valleys) and tops (mountains). Finally the residue of *nlg*-transformation f_{nlg} is analysed by local fractal analysis f_{FD} and multi-fractal dimension f_{MF} (Sarkar and Chaudhuri, 1994). For each pixel a local fractal dimension is calculated.

From the three images original f, *nlg* residue f_{nlg} and opening-closing residue f_{OF}, the measures listed in Table 2 were performed. Means ($m1$) and standard deviations (SD) ($m2$) from all points inside the area considered have dimension [*nm*]. Features from dark and bright areas allow the differentiation of surface changes in valleys, depressed regions, the dark areas, and on mountains, the bright areas. Features from f_{nlg} quantify the very fine scale variations and features from f_{OF} can reflect the slightly larger variations. Compared to Kempe et al. (2004), where lineal structures were examined (object-oriented), only isotropic variability was measured in the here presented investigations.

Classification

From each of the 251 topological AFM images 16 features were extracted. The data were grouped into 4 classes according to their sample location (supervised training approach). By means of a stepwise linear discrimination analysis (LDA) the most relevant features were selected to discriminate the defined classes. All classification results were jack-knifed (hold one out procedure) (procedures stepdisc, discrim, candisc, SAS V9.1.3, SAS Institute Inc., Carry, US). All statistical evaluations were done at 95% confidence level.

The 4-class scheme (subaquatic, intertidal, subaerial, Wadden) leads to unsatisfactory results. The subaquatic and intertidal samples were not distinguishable from each other and the total classification result was unacceptable. Hence, the assumption of similarity of the intertidal and the Wadden samples as partially watered specimen group could not be verified. Moreover, the distance between the sample locations at the Spanish coast is so small that an exchange of sand grains by wind and/or water and overprint of different processes could not be excluded. Hence, it was assumed that intertidal specimens display a mixture of grain patterns of subaquatic and subaerial origin. We have thus trained a 2-class classifier with the subaquatic and subaerial specimens only. The selected features were $m1b$, $m1d$, $m2mf$ and $m2b$, listed in decreasing importance. For feature descriptions, see Table 2.

This classifier was applied to the intertidal specimens resulting in a distinction of 45 cases as subaquatic and 27 cases as subaerial. The statistical quality of this classification with a mean probability of 94% $\pm$ 0.05 (range 73.7–100.0) for the subaquatic specimens is nearly perfect. The mean value of subaerial is 83.7% $\pm$ 0.13 (range 54.6–99.6) was reasonable which strengthens our assumption that intertidal specimens consist of two clusters similar to the subaquatic and subaerial specimen groups. Hence, the classified subgroups of intertidal origin were merged with the subaquatic and subaerial groups respectively (see Tables 1 and 3) named as subaquatic+ and subaerial+.

The classification result in the 3-class case (subaquatic+, subaerial+, Wadden) is shown in Table 4. The most discriminative feature is $m2b$, the standard deviation of the higher (brighter) areas in f_{nlg}, followed by the mean $m1b$ of the same and $m1d$, the mean of the prominent areas in f_{nlg}. Seemingly the most prominent regions of the surface (unhachted regions in Figure 5E) are subject to the changes found as discriminatable. Only surface structures in the range of 120 nm (*nlg*

TABLE 2
List of extracted features with their abbreviated names

Name	Description
m1, m2	mean, SD of f_{nlg} (whole area)
m1d, m2d	mean, SD of f_{nlg} (dark area, depressed regions)
m1b, m2b	mean, SD of f_{nlg} (bright area, prominent regions)
m1f, m2f	mean, SD of f_{OF} (whole area)
m1fr, m2fr	mean, SD of local fractal dimension (FD)
m1mf, m2mf	mean, SD of local multi-FD
mo1d, mo2d	mean, SD of AFM height map f (bright area)
mo1b, mo2b	mean, SD of AFM height map f (dark area)

TABLE 3
Analyzed (grouped) digital image data consisting of original subaquatic, subaerial and Wadden data combined with the classified intertidal data (see Table 1)

Code	Type	Location	Images	Resolution [nm/pixel]	Total Area [μm^2]
1	subaquatic+	Gibraltar	49 + 45 = 94	58.5	37600
3	subaerial+	Gibraltar	68 + 27 = 95	58.5	38000
4	Wadden	North Sea	62	58.65/39.1	24800

TABLE 4
Number of observations and percent classified into respective classes (1 = subaquatic+, 3 = subaerial+, 4 = Wadden)

From Class	1	3	4	Total	%
1	65	1	28	94	69.15
3	0	77	18	95	81.10
4	16	5	41	62	66.10
Total				251	72.90

transformation) showed differences. The overall classification rate was 72.9%. The data points are plotted via the first and second canonical variables in Figure 6.

The latter represents the best view into the feature space under all linear combinations of the measured features for discrimination of the three classes. It can be recognised that class 3 (blue, subaerial+) can be discriminated best from the others. Class 1 (red, subaquatic+) and 4 (green) show a large overlap. The features and hence the scanned surfaces are more frequent similar to each other than to class 3. Assuming wind and hence grain-to-grain interaction in the subaerial samples, and water influence for the other groups let suspect that the main difference in alterations on grain surfaces is water related. The size of magnitude of surface changes found important for discrimination is nearly one less than the etch marks (Kempe et al. 2004) reflecting mechanical influences.

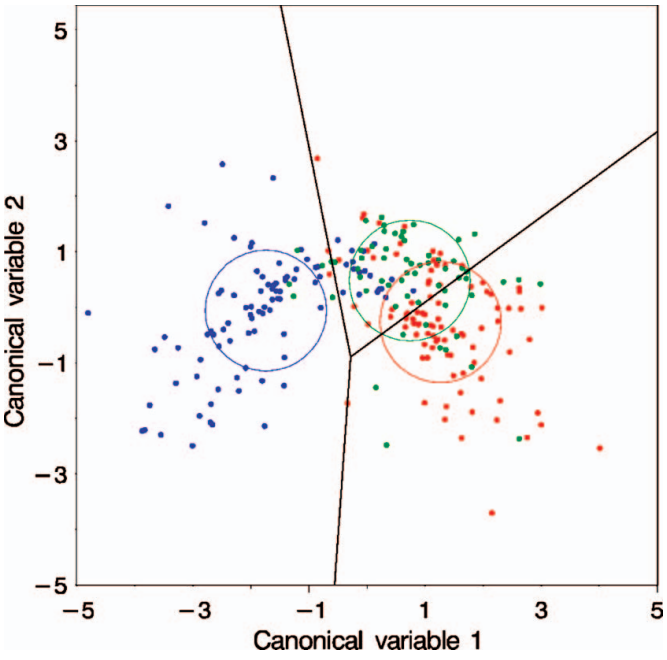

FIG. 6. Classification into the classes 1 (red, subaquatic+, Gibraltar), 3 (blue, subaerial+, Gibraltar) and 4 (green, Wadden, North Sea) with circles of variance 1 and discrimination function.

DISCUSSION

Much effort is needed in order to differentiate between individual morphologies and morphotypes created on rock surfaces and mineral grain surfaces by different media and processes. The materials presented here are a first approach to quantitatively measure and characterise wear down features of rock and mineral surfaces based on topographic AFM data. The ultimate goal is to create a database for differentiating between biogenic and abiogenic morphogenetic processes and the morphological patterns created by their course of action on the nanoscale. Whether these changes of mineral surfaces are biofilm products or mere physical/chemical products is of high importance for many environments and technical methods.

Using mainly sand grains exposed to different erosive and corrosive forces and pathways we mathematically characterised the deformations created by the individual processes. SEM-microphotographs serve as a general orientation, while AFM-micrographs were used for measurements and computing on the nano- to microscale. The analysis proves, that it ultimately will be possible to assign certain sets of profiles and surface morphologies to biological, chemical or physical impact on mineral surfaces. Of course, it should also be investigated at a later stage, whether the recognised patterns depend on the corroding medium alone or to some degree also on the mineralogy. It could be speculated that biological and physical processes leave their overlapping imprints at various proportions, in relationship to the chemical and physical properties, crystallographic-lattice, and nutrient properties of particular minerals. Once this technology is further elaborated, it may be possible to analyse surface sections of extraterrestrial rocks and minerals, even in outcrops, for ancient or extant biopitting activities as contrasted by image analyses to merely chemical or physical factors.

An essential feature for the separation of morphological alterations under subaerial versus subaquatic conditions are the changes in elevated surface areas (Figure 5E) and especially the positive changes in Figure 5. Consequently, however, the changes in Figure 5D can only be attributed to the non-hatched areas of Figure 5E. A general assumption is, that physical contact of grain to grain, must be more marked (sharp edges, triangular breaks) than the action of water (and other solvents) or of biological forces (chemical and physical). The empirical findings of Gehrmann (1992) and Krumbein (1969) correspond well with this assumption as further elaborated by Sterflinger and Krumbein (1997). However, physical, i.e. mechanical action executed by biofilms (Dornieden et al. 2000) and combined physical and chemical action as documented by Brehm et al. (2005) may bridge the gap partially.

So far, only chemical action of microorganisms in biocorrosion of mineral and rock material has been considered. Physical or mechanical action of microorganisms was not expected to occur. This smoothening or soft action is documented by our measurements on 100 nm scale. However, larger scale variations of micromorphology as documented by Brehm et al. (2005), where even grain diminution and grain partitioning creating

smaller grain size distributions as compared to sterile controls was demonstrated, so far remain outside our approach. On the nanometer scale, however, the results give concrete and encouraging evidence of a standardised discrimination potential regarding physical and chemical actions of microorganisms as compared to pure physical and chemical actions of environmental physics and chemistry. Life shapes differently as compared to inanimate causes and products.

It is perhaps possible within the fractal (i.e., scale invariant) range to mathematically differentiate between the impact of non-living physical (sand grain and sand grain collision) or chemical (etching of crystal surfaces along the crystal lattice) attack and shaping of surfaces through microbial physical or chemical influences. These may perhaps be compared to the antique Greek and Roman sculpturing of statues where the impression of the elegant curvature of human body is genially achieved by artists. Smoothness and impact of living cells or their metabolic products certainly differ from meteorologically derived brutal impacts. Our data allow such differentiation at least in the scale between 100 and 500 nanometers.

Nanotechnologies in material sciences and mineral exploration demand for careful optical and mathematical treatment of micromorphologies. The analytical technology of precise measurement and discrimination between biogenic and purely physical/chemically produced transects across mineral grain surfaces is only in its infancy. It may however evolve into a powerful tool for industrial analysis of corrosion and biocorrosion and general for interpretation of terrestrial and extraterrestrial geomorphogenetic patterns versus biogeomorphogenetic ones. The latter will certainly give deeper insight into terrestrial geochemical and biogeochemical processes as well as to unravelling the history of sedimentary rocks. Moreover it can also serve as a tool for extraterrestrial discriminants helping to define borders and detect traces of life (Horneck et al. 2008; Krumbein 2008; Altermann 2009).

CONCLUSIONS

In this work we discuss a mathematical procedure to classify surface alterations of rocks and mineral grains based on topographic data obtained with an atomic force microscope. In a step-by-step approach from general imaging via light microscopy (LM), scanning electron microscopy (SEM) and finally, precise three-dimensional atomic force microscopy (AFM) quantitative data of the surface morphology is obtained. For classification, we suggest a set of image analytical methods to characterize morphogenetic patterns on aquatic and terrestrial rock and mineral surfaces. With this approach physical/chemical (etching and collision) abrasion patterns can be differentiated from biological erosion and corrosion (grain diminution, biopitting). Thus, it is well possible to differentiate between surface changes dominated by subaerial, subaquatic and by biological impact. The mathematical approach might equally be used for the detection of aeolian, subaquatic, and biological modification of sedimentary grains and rock surfaces in terrestrial and extraterrestrial environments and for the investigations of environmental damage to sculptures, monuments and architectural constructions.

REFERENCES

Altermann W. 1986. The Upper Paleozoic pebbly mudstone facies of Peninsular Thailand and Western Malaysia—Continental margin deposits of Paleoeurasia. Geol Rdsch 75(2):79–89.

Altermann, W. 2007. The early Earth's record of enigmatic cyanobacteria and supposed extremophilic bacteria at 3.8 to 2.5 Ga. In. J Seckbach (Ed), Algae and Cyanobacteria in Extreme Environments. Cellular Origin, Life in Extreme Habitats and Astrobiology (COLE) 11, Dordrecht: Springer Verlag. P 759–778.

Altermann W. 2009. Introduction to from fossils to astrobiology—A roadmap to a fata morgana? In J. Seckbach and M. Walsh (eds.), From Fossils to Astrobiology, volume 12 of COLE, pp. xv–xxvii. Springer: Dordrecht.

Altermann W, Böhmer C, Gitter F, Heimann F, Heller I, Läuchli B, Putz C. 2009. Defining biominerals and organominerals. direct and indirect indicators of life. Discussion. Sediment Geol 213:150–151.

Altermann W, Herbig H-G. 1991. Tidal at deposits of the lower Proterozoic Campbell Group along the southwestern margin of the Kaapvaal craton, Northern Cape Province, South Africa. J Afr Earth Sci 13:415–435.

Aurich V, Weule J. 1995. Non-linear Gaussian filters performing edge preserving diffusion. In Proc. 17. DAGM-Symposium. Springer, Bielefeld, 10: 538–545.

Bates RL, Jackson JA. (eds) 1990. Glossary of Geology. New York: American Geological Institute, Virginia, 788p.

Benzerara K, Hyun Yoon T, Menguy N, Tyliszczak T, Brown G. 2005. Nanoscale environments associated with bioweathering of a Mg-Fe pyroxene. In Proceedings of the National Academy of Sciences of the United States of America (PNAS) 102:979–982.

Brasier M, McLoughlin N, Green O, Wacey D. 2006. A fresh look at the fossil evidence for early Archean cellular life. Phil Trans Roy Soc **361**(B): 887–902.

Brehm U, Gorbushina AA, Mottershead D. 2005. The role of microorganisms and biofilms in the breakdown and dissolution of quartz and glass. Palaeogeogr Palaeoclimat Palaeoecol 219:117–129.

Cailleux A. 1952. Morphoskopische Analyse der Geschiebe und Sandkörner und ihre Bedeutung für die Paläoklimatologie. Geol Rundsch 40:11–19.

Carter NEA, Naylor LA, Viles HA. 2001. Biogeomorphology revisited: present and future pathways for understanding the relationships between organisms and the landscape. In: R. G. Society (ed.), Royal Geographical Society/ Institute of British Geographers Annual Conference, Abstracts. Plymouth. P 116.

Civan F. 2006. Pitting during crystal dissolution: Modeling and analysis. Encyclopedia of Surface and Colloid Science. Taylor and Francis, New York.

Danin G, Garty J. 1983. Distribution of cyanobacteria and lichens on hillsides of the Negev highlands and their impact on biogenic weathering. Z Geomorph NF 27:423–444.

Danin G, Gerson R, Marton K, Garty J. 1982. Patterns of limestone and dolomite weathering by lichens and blue-green algae and their palaeoclimatic significance. Palaeogeogr Palaeoclimatol Palaeoecol 37:221–233.

Dornieden T, Gorbushina AA, Krumbein WE. 1997. Änderungen der physikalischen Eigenschaften von Marmor durch Pilzbewuchs. Int J Restor Buildings Monuments 3:441–456.

Dornieden T, Gorbushina AA, Krumbein WE. 2000. Patina- physical and chemical interactions of sub-aerial biofilms with objects of art. In: O. Ciferri, G. Mastromei, and P. Tiano (eds.), Of Microbes and Art. The role of microbial communities in the degradation and protection of cultural heritage. Kluwer, Dordrecht. P 105–119.

Einen J, Krober C, Ovreas L, Thorseth I, Torsvis T. 2004. Biodegradation of basaltic glass—An experimental approach. In International Workshop in Geomicrobiology "A Reserach Area in Progress," Program and Abstract Vol., Univ. Aarhus, Denmark. P 55.

Eppard, M., Krumbein, W. E., Koch, C., Rhiel, E., Staley, J., and Stackebrandt, E. 1996. Morphological, physiological and molecular biolocal investigation on new isolates similar to the genus geodermatopilus (actinomycetes). Arch Microbiol 166:12–22.

Flügel E. 2004. Microfacies of carbonate rocks: analysis, interpretation and application. Springer, Berlin, Heidelberg, New York. 976 pp.

Fortuin AR. 1984. Late Ordovician glaciomarine deposits (Orea shale) in the Sierra de Albarracin, Spain. Palaeogeography Palaeoclimat Palaeoecol (3-Papaeo) 48:245–261.

Furnes H, Banerjee N, Muehlenbachs K, Staudigel H, de Wit MJ. 2004. Early life recorded in Archean pillow lavas. Science 304:578–581.

Furnes H, Muehlenbachs K, Tumyr O, Torsvik T, Thorseth IH. 1999. Depth of active bio-alteration in the ocean crust: Costa Rica Rift (hole 504b). Terra Nova 11:228–233.

Fuxing W, Junfa CJH, Jing JLHJW. 1993. Biocarst. Geol. Publ. House, Beijing.

Gehrmann CK. 1992. Endolithic lichens and the corrosion of carbonate rocks - a study of biopitting. Int J Mycol Lichenol 5:37–48.

Gehrmann CK, Krumbein WE. 1994. Interactions between epilithic and endolithic lichens and carbonate rocks. In HF Ott and F Zezza (eds.), Proc. 3rd Int. Conf. on the conservation of monuments in the Mediterranean Basin, Soperintendanza ai Beni Artistici e Storice, Venice. P 311–316.

Gehrmann CK, Krumbein WE, Petersen K. 1988a. Lichen weathering activities on mineral and rock surfaces. Studia Geobotanica 8:33–45.

Gehrmann CK, Petersen K, Krumbein WE. 1988b. Silicole and calcicole lichens on Jewish tombstones–Interactions with the environment and biocorrosion. In Vith International Congress on Deterioration and Conservation of Stone, 12.-14.09.1988, pp. 33-38, Nicolas Copernicus University, Torun, Poland.

Gorbushina AA, Boettcher M, Brumsack H-J, Krumbein WE, Vendrell-Saz M. 2001. Biogenic forsterite and opal as a product of biodeterioration and lichen stromatolite formation in table mountain systems (tepuis) of Venezuela. Geomicrobiol J 18:1–17.

Gorbushina AA, Krumbein WE. 2000. Subaerial microbial mats and their effects on soil and rock. In RE Riding and SM Awramik (eds.), Microbial Sediments. Springer, Berlin. P 161–170.

Gorbushina AA, Krumbein WE, Panina L, Soukharjevsk S, Wollenzien U. 1993. On the role of black fungi in colour change and biodeterioration of antique marbles. Geomicrobiol J 11:205–221.

Gorbushina AA, Krumbein WE, Vlasov D. 1996. Biocarst cycles on monument surfaces. In R. Pancella (ed.), Preservation and restoration of cultural heritage. Proceedings of the 1995 LPC Congress, EPFL, Lausanne. P 319–322.

Hoffland E, Kuyper TW, Wallander H, Plassard C, Gorbushina AA, Haselwandter K, Holmström S, Landeweert R, Lundström US, Rosling A, Sen R, Smits MM, van Hees PAW, van Breemen N. (2004) The role of fungi in weathering. Front Ecol Environ 2(5):258–264.

Horneck G, Stöffler D, Ott S, Hornemann U, Cockell C, Moeller R, Meyer C, de Vera J, Fritz J, Schade S, Artemieva NA. 2008. Microbial rock inhabitants survive hypervelocity impacts on Mars-like host planets: First phase of lithopanspermia experimentally tested. Astrobiology 8:17–44.

Kempe, A. 2003. Entwicklung einer neuen Präparationsmethode und Untersuchung verkieselter Mikrofossilien des Präkambriums mit Hilfe der Rasterkraft- und Elektronenmikroskopie. PhD thesis, LMU München: Fakultät für Geowissenschaften.

Kempe A, Jamitzky F, Altermann W, Baisch B, Markert T, Heckl M. 2004. Discrimination of aqueous and aeolian paleoenvironments by atomic force microscopy—A database for the characterization of martian sediments. Astrobiology 4:51–64.

Krinsley D, Doornkamp JC. 1973. Atlas of Quartz Sand Surface Textures. Cambridge University Press, Cambridge, UK.

Krumbein WE. 1969. Über den Einfluss der Mikroflora auf die exogene Dynamik (Verwitterung und Krustenbildung). Geol Rdsch 58:333–363.

Krumbein WE. 1987. Die Entdeckung inselbildender Mikroorganismen. In: G Gerdes, WE Krumbein, and H-E Reineck (eds.), Mellum - Portrait einer Insel. Kramer, Frankfurt am Main.

Krumbein WE. 2003. Patina and cultural heritage - a geomicrobiologist's perspective. In: R. Kozlowski (ed.), Proceedings of the Vth EC Conference Cultural Heritage Research: A Pan-European Challenge, Krakow. EC and ISC. P 39–47.

Krumbein WE. 2008. Biogenerated rocks and rock structures. Space Sci Rev 135:81–94.

Krumbein WE, Gorbushina AA. 1995. On the interaction of water repellent treatments of building surfaces with organic pollution, micro organisms and microbial communities. In: F Wittmann, T Siemes, L Verhoef (eds), Surface treatment of building materials with water repellent agents. Delft University of Technology, Delft. P 29-1–29-10.

Krumbein WE, Gorbushina AA, Palinska KA, Sterflinger K. 1998. The paradoxon of glass. stability and decay; biological deterioration and transformation; conservation and restoration. In: R Lefevre and I Pallot-Froissard (eds.), Les Materiaux Vitreux: Verre et Vitraux. Edipuglia, Bari. P 107–124.

Krumbein WE, Jens K. 1981. Biogenic rock varnishes of the Negev desert (Israel) an ecological study of iron and manganese transformation by cyanobacteria and fungi. Oecologia 50:25–38.

Krumbein WE, Paterson DM, Zavarzin GA (Eds.), GAZ. 2003. Fossil and Recent Biofilms—A natural history of Life on Earth. Kluwer Academic Publishers, Dordrecht.

Krumbein WE, Paterson DM, Stal LJE. 1994. Biostabilization of Sediments. BIS-Verlag, Oldenburg, 529p.

Krumbein WE, Urzi CE, Gehrmann C. 1991. On the biocorrosion and biodeterioration of antique and mediaeval glass. Geomicrobiol J 9:139–160.

Kuenen Ph.H. 1959a. Experimental abrasion 3. Fluviatile action on sand: Am J Sci 257:172–190.

Kuenen Ph.H. 1959b. Sand—Its origin, transportation and accumulation. Geol. Soc. S. Africa, Alexandre du Toit memorial Lecture, no 6, 33p.

Kuenen PhH. Perdok WG. 1962. Experimental abrasion 5. Frosting and defrosting of quartz grains. J. Geol 70:648–658.

Marshall JR. (edit.) 1987. Clastic Particles: Scanning Electron Microscopy and Shape Analysis of Sedimentary and Volcanic Clasts. Van Nostrand-Reinhold, New York, 347pp.

Rasband WS. 1997–2009. ImageJ, U. S. National Institutes of Health, Bethesda, Maryland, USA.

Rodenacker K, Bengtsson E. 2003. A feature set for cytometry on digitized microscopic images. Anal Cell Pathol 25:1–36.

Sarkar N, Chaudhuri BB. 1994. An efficient differential boxcounting approach to compute fractal dimensions of images. IEEE Trans Syst Man Cybernetics 24:115–120.

Schieber J, Bose P, Eriksson PG, Banerjee S, Sarkar S, Altermann W, Catuneanu OE. 2007. Atlas of microbial mat features preserved within the siliciclastic rock record, vol. 2 Atlases in Geosciences. Elsevier. 311pp.

Serra J. 1982. Image analysis and mathematical morphology. Academic Press Inc., London.

Staley JT, Palmer F, Adams JB. 1982. Microcolonial fungi, common inhabitants on desert rocks? Science 215:1093–1095.

Sterflinger K, Krumbein WE. 1995. Multiple stress factors affecting growth of rock inhabiting black fungi. Botan Acta 108:490–496.

Sterflinger K, Krumbein WE. 1997. Dematiaceous fungi as the main agent of biopitting on mediterranean marbles and limestones. Geomicrobiol J 22:219–231.

Stroncik NA, Schmincke HU. 2002. Palagonite—A review. Int J Earth Sci (Geol. Rundsch.) 91:680–697.

Thorseth IH, Furnes H, Tumyr O. 1995. Textural and chemical effects of bacterial activity on basaltic glass: an experimental approach. Chem Geol 119:139–160.

Tietz G. 2006. Lösung oder neuerliches Wachstum auf Quarzkörnern: ein Indikator chemischer Verwitterung unter tropischen Klimabedingungen. Zbl Geol Paläont Teil 1–1. 151–171.

Viles HA. 1988. Cyanobacterial and other biological influence on terrestrial limestone weathering on Aldabra. Proc Biol Soc Wash 8:23–31.

Viles HA, Goudie A. 2000. Weathering, geomorphology and climatic variability in the central Namib desert. In: SJ McLaren and DR Kniveton (eds.), Linking climate change to land surface change. Kluwer, Dordrecht. P 65–82.

Whalley WB, Krinsley DH. 1974. A scanning electron microscope study of surface textures of quartz grains from glacial environments. Sedimentology 21:87–105.

Winkler G, Aurich V, Hahn KR, Martin A, Rodenacker K. 1999. Noise reduction in images: Some recent edge-preserving methods. Pattern Recognition and Image Analysis: Advan Math Theory Applications 9:749–766.

Zhang X-G, Pratt BR. 2008. Microborings in early cambrian phosphatic and phospatized fossils. Paleogeogr Paleoclimatol Paleoecol 267:185–195.